Molecule Glue Profiling Unveils the Dynamics of KRAS-Induced Proximity

Zhaoxia Yin, Xiaojian Wang and Tiejun Bing

ICE Bioscience, INC. Building 16, Yard 18, Kechuang 13th Street, Beijing, 100176
bingtj@ice-biosci.com

ICE Bioscience
Innovative CRO+Explorer

Abstract Number:

INTRODUCTION

KRAS molecular glues inhibit KRAS activity by binding to cellular chaperone proteins (such as cyclophilin A, CYPA) to form a ternary complex. The formation of this ternary complex not only blocks the RAS/RAF signaling pathway but also blocks the RAS/SOS1 and RAS/PI3K signaling pathways, thus demonstrating superior inhibitory activity compared to small-molecule inhibitors. Our integrated platform employs advanced in vitro assays to explore these KRAS molecular glues, including KRAS/CYPA ternary complex assay, KRAS(ON)/CYPA/cRAF binding assay, 2D/3D cell proliferation assay, ERK phosphorylation detection, and cellular NanoBRET assay for RAS-RAF disruption. It also includes a p-ERK panel and a 2D/3D cell panel. Overall, we provide a comprehensive platform for the screening and evaluation of KRAS molecular glues, offering a scientific basis for the clinical application of KRAS molecular glues.

1. KRAS (ON)/CypA Ternary assay by HTRF

Molecular glues(MG) can induce the formation of a ternary complex between KRAS and CYPA. The detection of this ternary complex formation using the HTRF method facilitates high-throughput screening for KRAS molecular glues.

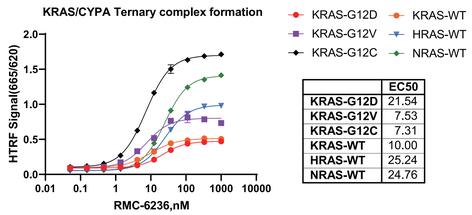

	EC50
KRAS-G12D	21.54
KRAS-G12V	7.53
KRAS-G12C	7.31
KRAS-WT	10.00
HRAS-WT	25.24
NRAS-WT	24.76

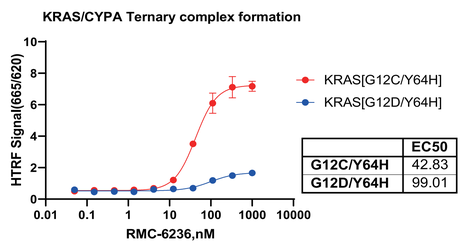

	EC50
G12C/Y64H	42.83
G12D/Y64H	99.01

Figure 1: KRAS (ON)/CypA ternary complex formation by HTRF. KRAS molecular glue RMC-6236 induces the formation of ternary complexes between KRAS wild-type and various mutants with CYPA.

2. KRAS(ON)/CypA/cRAF binding assay by HTRF

Molecular glues induce the formation of a ternary complex between KRAS and CYPA, thereby inhibiting the binding of cRAF, SOS1, or PI3K p110α to KRAS and blocking downstream signaling pathways. The mutual binding between cRAF , SOS1 or PI3K and KRAS can be detected by HTRF.

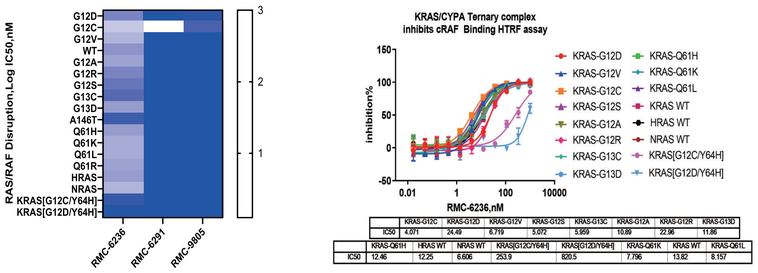

	KRAS-G12C	KRAS-G12D	KRAS-G12V	KRAS-G12S	KRAS-G13C	KRAS-G12A	KRAS-G12R	KRAS-G13D
IC50	4.071	24.49	6.719	5.072	5.959	10.89	22.96	11.86

	KRAS-Q61H	HRAS WT	NRAS WT	KRAS[G12C/Y64H]	KRAS[G12D/Y64H]	KRAS-Q61K	KRAS WT	KRAS-Q61L
IC50	12.46	12.25	6.606	253.9	820.5	7.796	13.82	8.157

Figure 2: KRAS(ON)/CypA/cRAF binding assay by HTRF. RMC-6236 showed potent inhibition against single KRAS mutants in the RAS/RAF blockade assay, but its activity was markedly weaker against the double mutants KRAS[G12C/Y64H] and KRAS[G12D/Y64H], suggesting that these dual mutations may confer resistance to RMC-6236.

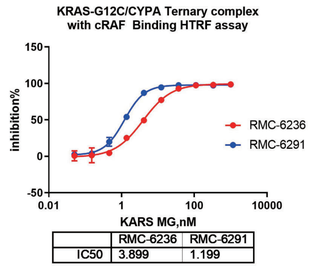

	RMC-6236	RMC-6291
IC50	3.899	1.199

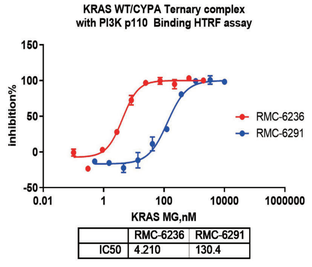

	RMC-6236	RMC-6291
IC50	4.210	130.4

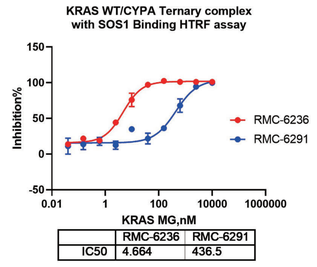

	RMC-6236	RMC-6291
IC50	4.664	436.5

Figure 3: KRAS(ON)/CypA/cRAF, SOS1 or PI3K binding assay by HTRF. The results confirm that KRAS molecular glues not only inhibit the RAS/RAF pathway but also block the RAS/SOS1 and RAS/PI3K signaling pathways.

3. KRAS MG/CypA/KRAS binary and ternary assay by SPR

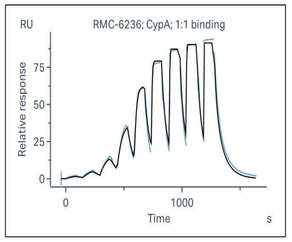

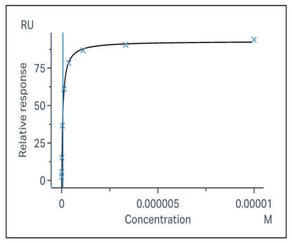

1.52 4.57 13.72 41.15 123.46 370.37 1111.11 3333.33 10000 nM

Immobilized ligand	Injection variables Single cycle kinetics 1 Solution	Kinetics model	1:1 binding ka (1/Ms)	kd (1/s)	KD (M)	Rmax (RU)	Quality Kinetics Chi² (RU²)	U-value	Affinity model	Steady state affinity KD (M)	Rmax (RU)
CypA	RMC-6236	1:1 binding	7.03e+05	4.16e-02	5.92e-08	91.9	6.75e+00	5	Steady state affinity	6.50e-08	93.2

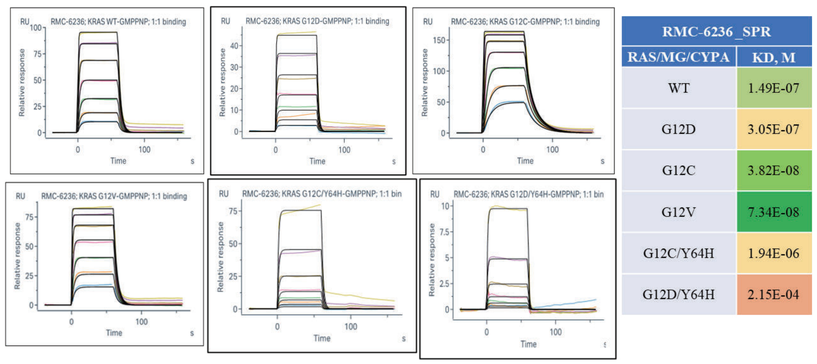

RMC-6236_SPR	
RAS/MG/CYPA	KD, M
WT	1.49E-07
G12D	3.05E-07
G12C	3.82E-08
G12V	7.34E-08
G12C/Y64H	1.94E-06
G12D/Y64H	2.15E-04

Figure 4. SPR-based affinity profiling of RMC-6236 for the RAS/CYPA interaction. a. Binding kinetics of RMC-6236 to CYPA alone. b. Affinity measurements of RMC-6236-induced ternary complexes of RAS–CYPA across distinct RAS mutants.

4. Cell based assay

NanoBRET assay is developed to investigate whether KRAS molecular glue can induce the formation of a KRAS/MG/-CYPA ternary complex within cells, which in turn inhibits the binding of RAS to RAF.

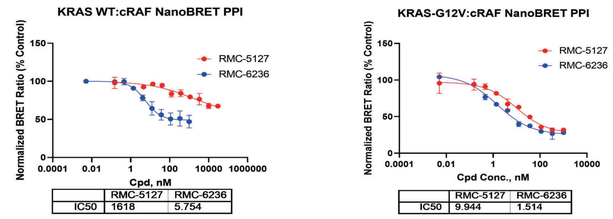

	RMC-5127	RMC-6236
IC50	1618	5.754

	RMC-5127	RMC-6236
IC50	9.944	1.514

Figure 5: Cellular NanoBRET PPI assay. The results show that RMC-6236 and RMC-5127 formed ternary complexes within cells, thereby blocking the binding of effector proteins to KRAS WT or G12V, and thus inhibiting downstream signaling. RMC-5127 exhibited selectivity for KRAS G12V.

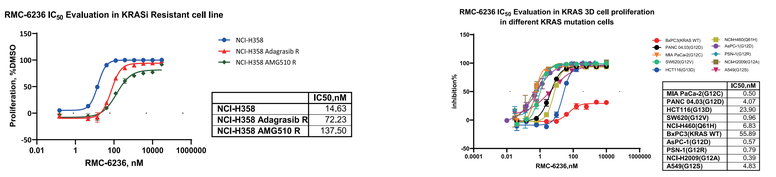

	IC50,nM
NCI-H358	14.63
NCI-H358 Adagrasib R	72.23
NCI-H358 AMG510 R	137.50

	IC50,nM
MIA PaCa-2(G12C)	0.50
PANC 04.03(G12D)	4.07
HCT116(G13D)	23.90
SW620(G12V)	0.96
NCI-H460(Q61H)	6.83
BxPC3(KRAS WT)	55.89
AsPC-1(G12D)	0.57
PSN-1(G12R)	0.79
NCI-H2009(G12A)	0.39
A549(G12S)	4.83

Figure 6. Cell proliferation assay for the IC50 evaluation of RMC-6236 in resistant cell lines(a) and different KRAS mutation cell lines(b), and pERK detection in different KRAS mutation cell lines(c), results suggests that the compound does not exhibit significant resistance, and can inhibit a broader spectrum of KRAS-mutated tumor cells compared to other small molecule inhibitors.

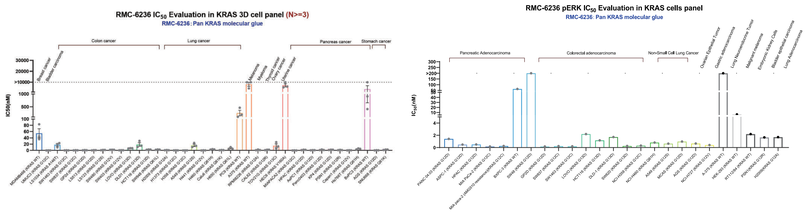

Figure 7. The IC50 evaluation of KRAS MG across a panel of 3D cultured Pan KRAS cell lines(a) and pERK panel(b). The results indicate that RMC-6236, as a molecular glue, can inhibit a broader spectrum of KRAS-mutated tumor cells compared to other small molecule inhibitors.

Data Summary

Assay Formation	RMC-6236, IC50, nM												
KRAS mutation	WT	G12V	G12C	G12D	G12S	G13C	G13D	Q61H	Q61K	Q61L	HRAS	NRAS	G12C/Y64H	G12D/Y64H
KRAS(ON)/CypATernary assay by HTRF	2.57	1.86	3.60	9.97	-	-	-	-	-	-	25.13	28.23	42.83	99.01
KRAS(ON)/CypA/cRAF binding assay by HTRF	13.82	6.72	4.07	24.49	5.07	5.96	11.86	12.46	7.80	8.16	12.25	6.61	253.9	820.5
Ternary assay by SPR_Kd,M	1.49E-07	7.34E-08	3.82E-08	3.05E-07	-	-	-	-	-	-	-	-	1.94E-06	2.15E-04
KRAS: cRAFNanoBRET PPI	5.74	1.51	-	-	-	-	-	-	-	-	-	-	-	-
3D cell proliferation	55.89	0.96	0.50	4.07	4.83	-	23.90	6.83	-	-	-	-	-	-
p-ERK detection	8.69	0.24	0.17	1.47	-	-	1.13	0.73						